

Holographic Dark Energy with Cosmological Constant

Yazhou Hu,^{a,b,c} **Miao Li**,^{c,a,1} **Nan Li**,^{a,b,c} **Zhenhui Zhang**,^{a,b,c,1}

^aState Key Laboratory of Theoretical Physics, Institute of Theoretical Physics, Chinese Academy of Sciences, Beijing, 100190

^bKavli Institute for Theoretical Physics China, Chinese Academy of Sciences, Beijing, 100190

^cSchool of Astronomy and Space Science, Sun Yat-Sen University, Guangzhou 510275, People's Republic of China

E-mail: asiahu@itp.ac.cn, mli@itp.ac.cn, linan@itp.ac.cn,
zhangzhh@mail.ustc.edu.cn

Abstract. Inspired by the multiverse scenario, we study a heterotic dark energy model in which there are two parts, the first being the cosmological constant and the second being the holographic dark energy, thus this model is named the Λ HDE model. By studying the Λ HDE model theoretically, we find that the parameters d and Ω_{hde} are divided into a few domains in which the fate of the universe is quite different. We investigate dynamical behaviors of this model, and especially the future evolution of the universe. We perform fitting analysis on the cosmological parameters in the Λ HDE model by using the recent observational data. We find the model yields $\chi^2_{\min} = 426.27$ when constrained by Planck + SNLS3 + BAO + HST, comparable to the results of the HDE model (428.20) and the concordant Λ CDM model (431.35). At 68.3% CL, we obtain $-0.07 < \Omega_{\Lambda 0} < 0.68$ and correspondingly $0.04 < \Omega_{hde0} < 0.79$, implying at present there is considerable degeneracy between the holographic dark energy and cosmological constant components in the Λ HDE model.

¹Corresponding author.

Contents

1	Introduction	1
2	ΛHDE Model: Theoretical Analysis	3
2.1	HDE with Cosmological Constant	3
2.2	Evolution Equations of $E(z)$ and $\Omega_{hde}(z)$	4
2.3	Dark Energy Equation of State	5
2.4	The Fate of the Universe in Λ HDE Model	5
3	The Observational Data and Methodology	7
4	Dynamical Behaviors and the Cosmic Expansion History	8
4.1	Fitting Results	8
4.2	The Expansion History	10
4.3	Equation of State	12
5	Conclusion	12
6	Appendix: Proof for $\log a$ not having a maximum in ΛHDE model	13

1 Introduction

The holographic dark energy model (HDE) [1, 2] was motivated by the holographic principle [3], as one of promising models to solve the nature of dark energy [4, 5]. The basic idea behind the HDE is that our universe is a sense finite and can be described by a two dimensional spherical holographic screen, thus there must be finite size effects, and one of these effects is the contribution to the zero point energy, depending on the size of the screen. Parametrically, this contribution assumes the form

$$\rho_{hde} = 3d^2 M_{pl}^2 L^{-2}, \quad (1.1)$$

where d is a dimensionless parameter to be determined by experiments, M_{pl} is the reduced Planck mass, and L denotes the size of holographic screen. For convenience, we work in the natural units, where $\hbar = c = 1$. In [2], one of the present authors suggested to choose the future event horizon of the universe as the size of the holographic screen, given by

$$R_h = a \int_t^{+\infty} \frac{dt}{a}. \quad (1.2)$$

This choice not only gives a reasonable value for the dark energy density, but also leads to an accelerated expansion.

The holographic dark energy (HDE) model based on Eq. (1.1) and Eq. (1.2) has proven to be a promising dark energy candidate. In the original paper [2], Li showed that the HDE can explain the coincidence problem. In [6], it is proven that the model is perturbatively stable. Other studies show that the model is in good agreement with the current cosmological observations [7]. Thus, the HDE model becomes one of the most competitive and popular dark energy candidates, and attracts a lot of interests [8].

It remains quite a mystery that to date all the papers on the HDE assume that dark energy is dominated by the HDE given by Eq.(1.1). In retrospect, this can be explained only by the reason that all the authors believed that the universe dominated by the HDE is the unique universe thus the form of dark energy is also unique. In the multiverse scenario, however, our observable universe is only one out of numerous universes, and the cosmological constant is one of the physics constants varying from one universe to another. Thus, it is not reasonable to simply assume it be vanishing.

Of cause, the modern multiverse scenario was motivated by the problem of dark energy. One of the present authors (ML) has recently been converted into a believer of the multiverse scenario by a quite different problem, namely the Fermi paradox. He now believes that the correct answer to the Fermi paradox is that our human being is the only intelligent being in our galaxy, possibly the only intelligent being in our universe, since it is really very difficult for an intelligent being to appear, the only reason for us to appear is that our universe is one out of numerous universe and it just happens that our universe is lucky enough, this is an anthropic answer to the Fermi paradox.

If for whatever reason that the multiverse scenario is true, then it is natural that the cosmological constant indeed is a constant to be determined by observations. On the other hand, the HDE on a general ground must be present too, according to the holographic principle. Thus, dark energy must consist of two parts, the first is a constant, the second is of the finite size effect. Indeed, in a calculation of the photon contribution to the zero point energy [9], it is found that in addition to the usual UV divergent part, there is a second divergent part proportional to L^{-2} where L is the radius of the de Sitter space. The usual quartically divergent part can be absorbed into the cosmological constant, the second part is the same form of the HDE. Thus, in general

$$\rho_{IR} = \Lambda + bM_{pl}^2L^{-2} + b_1L^{-4} + \dots . \quad (1.3)$$

It just happens that in our universe, the first term and the second term are comparable, and the third term is much smaller and can be neglected completely.

In this paper, we shall study this heterotic model of dark energy, in which there are the cosmological constant and the HDE. Thus we have

$$\rho_{de} = \rho_\Lambda + \rho_{hde}. \quad (1.4)$$

We shall name this model Λ HDE model. This model raises interesting theoretically questions: Is the CC positive or negative? If it is positive, whether it is greater or smaller than the HDE? Is the future of our universe dominated by the CC or by HDE? Will the big rip happen or not? In the rest of this paper, we shall try to answer these questions.

This paper is organized as follows. We study the Λ HDE model theoretically in Sect.II, and find that the parameters d and Ω_{hde} are divided into a few domains in which the fate of the universe is quite different. In Sect.III, we fit the model to the combined Planck + SNLS3 + BAO + HST and Planck + SNLS3 + BAO + HST + SDSS – Ly α datasets, and present the fittings results in Sec. IV. Many interesting issues, including the ratio of HDE and the equation of state (EoS) of the Λ HDE are discussed. Some concluding remarks are given in Sec. V. In this work, we assume today's scale factor $a_0 = 1$, so the redshift z satisfies $z = 1/a - 1$. The subscript “0” indicates the present value of the corresponding quantity unless otherwise specified.

2 Λ HDE Model: Theoretical Analysis

In this section, we will write down the basic equations for the Λ HDE model in a non-flat universe and study the fate of the universe in this model.

2.1 HDE with Cosmological Constant

In a spatially non-flat Friedmann-Robertson-Walker universe, the Friedmann equation can be written as

$$3M_{pl}^2 H^2 = \rho_{dm} + \rho_b + \rho_r + \rho_k + \rho_{de}, \quad (2.1)$$

where $\rho_k = -3M_{pl}^2 \frac{k}{a^2}$ is the effective energy density of the curvature component. In the Λ HDE model, the dark energy density is

$$\rho_{de} = \rho_\Lambda + \rho_{hde} = M_{pl}^2 \Lambda + 3M_{pl}^2 d^2 R_h^{-2}. \quad (2.2)$$

For convenience, we define the fractional energy densities of the various components, i.e.,

$$\Omega_k = \frac{-k}{H^2 a^2}, \quad \Omega_{de} = \frac{\rho_{de}}{\rho_c}, \quad \Omega_{hde} = \frac{\rho_{hde}}{\rho_c}, \quad \Omega_\Lambda = \frac{\rho_\Lambda}{\rho_c}, \quad \Omega_{dm} = \frac{\rho_{dm}}{\rho_c}, \quad \Omega_b = \frac{\rho_b}{\rho_c}, \quad \Omega_r = \frac{\rho_r}{\rho_c}, \quad (2.3)$$

where $\rho_c = 3M_{pl}^2 H^2$ is the critical density of the universe. The subscripts, “ k ”, “ de ”, “ hde ”, “ Λ ”, “ dm ”, “ b ” and “ r ” represent curvature, total dark energy, holographic dark energy, cosmological constant, dark matter, baryon and radiation, respectively. By definition, we have

$$\Omega_{hde} + \Omega_\Lambda + \Omega_{dm} + \Omega_b + \Omega_r + \Omega_k = 1. \quad (2.4)$$

The energy conservation equations for the components in the universe take the forms

$$\dot{\rho}_{hde} + 3H(\rho_{hde} + p_{hde}) = 0, \quad (2.5)$$

$$\dot{\rho}_\Lambda = 0, \quad \dot{\rho}_{dm} + 3H\rho_{dm} = 0, \quad \dot{\rho}_b + 3H\rho_b = 0, \quad \dot{\rho}_r + 4H\rho_r = 0, \quad \dot{\rho}_k + 2H\rho_k = 0. \quad (2.6)$$

Combining Eq. (2.5) and Eq. (2.6) together, we can obtain the form of p_{hde} ,

$$p_{hde} = -\frac{2}{3} \frac{\dot{H}}{H^2} \rho_c - \rho_c - \frac{1}{3} \rho_r + \frac{1}{3} \rho_k + \rho_\Lambda. \quad (2.7)$$

Substituting p_{hde} into Eq. (2.5), follow the similar procedure in Ref. [10], we get a differential equation of \dot{H} and $\dot{\Omega}_{hde}$:

$$2(\Omega_{hde} - 1) \frac{\dot{H}}{H} + \dot{\Omega}_{hde} + H(3\Omega_{hde} - 3 + 3\Omega_\Lambda + \Omega_k - \Omega_r) = 0. \quad (2.8)$$

From the energy density of the HDE in Eq. (1.1), we have

$$L = \frac{d}{H\sqrt{\Omega_{hde}}}. \quad (2.9)$$

Following Ref. [11], in a non-flat universe, the IR cut-off length scale L takes the form

$$L = ar(t), \quad (2.10)$$

and $r(t)$ satisfies

$$\int_0^{r(t)} \frac{dr}{\sqrt{1 - kr^2}} = \int_t^{+\infty} \frac{dt}{a(t)}. \quad (2.11)$$

By carrying out the integration, we find

$$r(t) = \frac{1}{\sqrt{|k|}} \text{sinn}\left(\sqrt{|k|} \int_t^{+\infty} \frac{dt}{a}\right) = \frac{1}{\sqrt{|k|}} \text{sinn}\left(\sqrt{|k|} \int_{a(t)}^{+\infty} \frac{da}{Ha^2}\right), \quad (2.12)$$

where the function $\text{sinn}(x)$ is defined as

$$\text{sinn}(x) = \begin{cases} \sin(x) & k > 0; \\ x & k = 0; \\ \sinh(x) & k < 0. \end{cases}$$

Equation (2.10) leads to another equation about $r(t)$, namely,

$$r(t) = \frac{L}{a} = \frac{d}{\sqrt{\Omega_{hde}} Ha}. \quad (2.13)$$

Combining Eqs. (2.12) and (2.13) yields

$$\sqrt{|k|} \int_t^{+\infty} \frac{dt}{a} = \arcsinn \frac{\sqrt{|k|} d}{\sqrt{\Omega_{hde}} a H}. \quad (2.14)$$

Taking derivative of Eq. (2.14) with respect to t , one gets

$$\frac{\dot{\Omega}_{hde}}{2\Omega_{hde}} + H + \frac{\dot{H}}{H} = \sqrt{\frac{\Omega_{hde} H^2}{d^2} - \frac{k}{a^2}}. \quad (2.15)$$

2.2 Evolution Equations of $E(z)$ and $\Omega_{hde}(z)$

Combining Eq. (2.8) with Eq. (2.15), we eventually obtain the following two equations governing the dynamical evolution of the Λ HDE model in a non-flat universe,

$$\frac{1}{E(z)} \frac{dE(z)}{dz} = -\frac{\Omega_{hde}}{1+z} \left(\frac{3\Omega_\Lambda + \Omega_k - \Omega_r - 3}{2\Omega_{hde}} + \frac{1}{2} + \sqrt{\frac{\Omega_{hde}}{d^2} + \Omega_k} \right), \quad (2.16)$$

$$\frac{d\Omega_{hde}}{dz} = -\frac{2\Omega_{hde}(1 - \Omega_{hde})}{1+z} \left(\sqrt{\frac{\Omega_{hde}}{d^2} + \Omega_k} + \frac{1}{2} - \frac{3\Omega_\Lambda + \Omega_k - \Omega_r}{2(1 - \Omega_{hde})} \right), \quad (2.17)$$

where $E(z) \equiv H(z)/H_0$ is the dimensionless Hubble expansion rate. Notice that we have

$$\Omega_k(z) = \frac{\Omega_{k0}(1+z)^2}{E(z)^2}, \quad \Omega_r(z) = \frac{\Omega_{r0}(1+z)^4}{E(z)^2}, \quad \Omega_\Lambda(z) = \frac{\Omega_{\Lambda0}}{E(z)^2}, \quad \Omega_b(z) = \frac{\Omega_{b0}(1+z)^3}{E(z)^2}, \quad (2.18)$$

and the fractional density of dark matter is given by $\Omega_{dm}(z) = 1 - \Omega_k(z) - \Omega_{hde}(z) - \Omega_\Lambda(z) - \Omega_r(z) - \Omega_b(z)$. Equations (2.16) and (2.17) can be solved numerically and will be used in the data analysis procedure.

2.3 Dark Energy Equation of State

The EoS of the HDE takes the form [12]

$$w_{\text{hde}} \equiv \frac{p_{\text{hde}}}{\rho_{\text{hde}}} = -\frac{1}{3} - \frac{2}{3}\sqrt{\frac{\Omega_{\text{hde}}}{d^2} + \Omega_k}. \quad (2.19)$$

So according to the partial pressure law, the EoS of the total dark energy is

$$w_{\text{de}} \equiv \frac{p_{\text{de}}}{\rho_{\text{de}}} = \frac{p_{\text{hde}} + p_{\Lambda}}{\rho_{\text{hde}} + \rho_{\Lambda}} = \frac{w_{\text{hde}}\Omega_{\text{hde}} - \Omega_{\Lambda}}{\Omega_{\text{hde}} + \Omega_{\Lambda}}. \quad (2.20)$$

Obviously the property of w_{de} is closely related to values of d and Ω_{Λ} .

2.4 The Fate of the Universe in Λ HDE Model

For convenience, we transform Eq. (2.1) into the following form

$$(1 - \Omega_{\text{hde}})H^2 = \Omega_{m0}H_0^2a^{-3} + \Omega_{r0}H_0^2a^{-4} + \Omega_{k0}H_0^2a^{-2} + \Omega_{\Lambda0}H_0^2, \quad (2.21)$$

and define

$$f(a) \equiv \Omega_{m0}H_0^2a^{-1} + \Omega_{r0}H_0^2a^{-2} + \Omega_{k0}H_0^2 + \Omega_{\Lambda0}H_0^2a^2. \quad (2.22)$$

Let $x \equiv \log a$, then we obtain

$$H = \sqrt{\frac{f(a)}{a^2(1 - \Omega_{\text{hde}})}}, \quad (2.23)$$

$$\frac{d}{dx} \ln \left| \frac{\Omega_{\text{hde}}}{1 - \Omega_{\text{hde}}} \right| + \frac{d}{dx} \ln |f(a)| = \frac{2}{d} \sqrt{\Omega_{\text{hde}} - (1 - \Omega_{\text{hde}}) \frac{kd^2}{f(a)}}. \quad (2.24)$$

Eq. (2.24) tells us how the HDE evolves with a . For simplicity, in this section we only study the $k = 0$ case. Then Eq. (2.24) becomes

$$\frac{d}{dx} \ln \left| \frac{\Omega_{\text{hde}}}{1 - \Omega_{\text{hde}}} \right| + \frac{d}{dx} \ln |f(a)| = \frac{2}{d} \sqrt{\Omega_{\text{hde}}}. \quad (2.25)$$

This equation can not be solved exactly. But for the purpose of studying the fate of the universe, we can introduce a good approximation.

During a period in which $f(a)$ is dominated by a single term on the right hand side of Eq. (2.22), we can use a constant k_r to approximate $\frac{d}{dx} \ln |f(a)|$. Then the Eq. (2.25) becomes

$$\frac{d}{dx} \ln \left| \frac{\Omega_{\text{hde}}}{1 - \Omega_{\text{hde}}} \right| = \frac{2}{d} \sqrt{\Omega_{\text{hde}}} - k_r. \quad (2.26)$$

It is easy to see that the cosmological constant term on the right hand side of Eq. (2.22) will dominate when scale factor a evolves to infinity. Thus we get $k_r = 2$ in this limit. Fortunately, it can be proved that a will always evolve to infinity. The proof is given in the appendix.

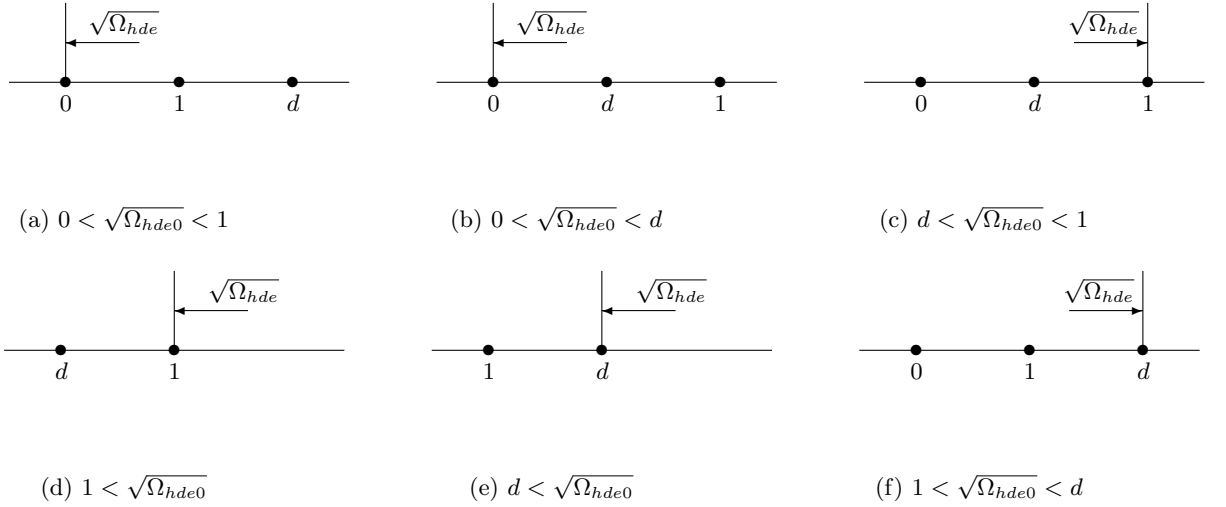


Figure 1. The evolution of $\sqrt{\Omega_{hde}}$ with different initial conditions.

With $k_r = 2$, we can rewrite the Eq. (2.26) and get its solution as follows:

$$\frac{d\Omega_{hde}}{dx} = \frac{2}{d}(\sqrt{\Omega_{hde}} - d)(1 - \Omega_{hde})\Omega_{hde}, \quad (2.27)$$

$$x + x_1 = \frac{d}{2d-2} \ln |1 - \sqrt{\Omega_{hde}}| - \frac{1}{(d^2-1)} \ln |\sqrt{\Omega_{hde}} - d| - \frac{1}{2} \ln \Omega_{hde} + \frac{d}{2d+2} \ln (1 + \sqrt{\Omega_{hde}}), \quad (2.28)$$

where x_1 is the constant of integration. Then let us exhibit how the HDE evolves:

The first three pictures in Fig.1 show how $\sqrt{\Omega_{hde}}$ evolves with the initial condition $\sqrt{\Omega_{hde0}} < 1$. In both picture(1a) and picture(1b), $\sqrt{\Omega_{hde0}} < d$, the right hand of Eq.(2.27) is negative, so $\sqrt{\Omega_{hde0}}$ will decrease with x . Thus the right hand of Eq.(2.27) will always be negative. So $\sqrt{\Omega_{hde0}}$ will keep decreasing to 0. According to Eq.(2.28) when $\sqrt{\Omega_{hde0}} \rightarrow 0^+$, $x \rightarrow +\infty$. Thus once $\sqrt{\Omega_{hde0}} < 1$, either $d < 1$ or $d > 1$, according to Eq.(2.23), H will always tend to a constant, which means space-time will be de Sitter in the future. In picture (1c), $d < \sqrt{\Omega_{hde0}} < 1$, the right hand of Eq.(2.27) is positive, so $\sqrt{\Omega_{hde0}}$ will increase with x . Thus the right hand of Eq.(2.27) will always be positive. $\sqrt{\Omega_{hde0}}$ will keep increasing to 1, according to Eq.(2.28) when $\sqrt{\Omega_{hde0}} \rightarrow 1^-$, $x \rightarrow +\infty$. So this solution describes a HDE dominated universe with big rip.

The last three pictures in Fig. 1 show how $\sqrt{\Omega_{hde}}$ evolves with the initial condition $\sqrt{\Omega_{hde0}} > 1$. In picture (1d), $\sqrt{\Omega_{hde0}} > d$, the right hand of Eq.(2.27) is negative, so when $d < 1$, the $\sqrt{\Omega_{hde0}}$ will keep decreasing with x all the way up to 1. According to Eq.(2.28) when $\sqrt{\Omega_{hde0}} \rightarrow 1^+$, $x \rightarrow +\infty$. So picture(1d) describes a HDE dominated universe with big rip. In picture(1e) (or in picture(1f)), $d < \sqrt{\Omega_{hde0}}$ (or $d > \sqrt{\Omega_{hde0}}$) the right hand of Eq.(2.27) will be negative (positive), so the $\sqrt{\Omega_{hde0}}$ will keep decreasing (or increasing) to d . According to Eq.(2.28), when $\sqrt{\Omega_{hde0}} \rightarrow d$, $x \rightarrow +\infty$. So they both describe an universe whose space-time will be de Sitter in the future.

3 The Observational Data and Methodology

We explore cosmological constraints on the Λ HDE model with the most recent observational data. For comparison, we will also present the fitting results of the original HDE and Λ CDM models. Data used in our analysis include:

- The SNLS3 combined sample [13, 14], consisting of 472 SNIa, combining the results of two light-curve fitting codes SiFTO [15] and SALT2 [16].¹ We follow the procedure of [25] and perform a complete analysis of the systematic errors. The χ^2 function takes the form

$$\chi_{SNLS3}^2 = \Delta \vec{\mathbf{m}}^T \cdot \mathbf{C}^{-1} \cdot \Delta \vec{\mathbf{m}}, \quad (3.1)$$

where \mathbf{C} is a 472×472 covariance matrix capturing the statistic and systematic uncertainties, and $\Delta \vec{\mathbf{m}} = \vec{\mathbf{m}}_B - \vec{\mathbf{m}}_{\text{mod}}$ is a vector of model residuals of the SNIa sample, with m_B the rest-frame peak B band magnitude of the SNIa and m_{mod} the predicted magnitude of the SNIa, given by

$$m_{\text{mod}} = 5 \log_{10} \mathcal{D}_L - \alpha(s - 1) + \beta \mathcal{C} + \mathcal{M}, \quad (3.2)$$

where \mathcal{D}_L is the Hubble-constant free luminosity distance, the stretch s is a measure of the shape of SN light-curve, \mathcal{C} is the color measure for the SN, and α, β are two nuisance parameters characterizing the stretch-luminosity and color-luminosity relationships, respectively. Following [13], we treat α and β as free parameters of χ^2 function.

- The Planck “distance priors” provided in [26], which are extracted from Planck first year [27, 28] observations. The data include the baryon component $\omega_b \equiv \Omega_b h^2$, the “acoustic scale” $l_a \equiv \pi r(z_*)/r_s(z_*)$, and the “shift parameter” $R \equiv \sqrt{\Omega_m H_0^2} r(z_*)$, where z_* is the redshift to the photon-decoupling surface [29], $r(z_*)$ is our comoving distance to z_* , and $r_s(z_*)$ is the comoving sound horizon at z_* . The distance priors provide an efficient summary of the CMB data in regards to dark energy constraints [30].
- The BAO data including the measurement of r_s/D_V at $z = 0.106$ from 6dFGS [31], the isotropic measurement of D_V/r_d at $z = 0.32$ from the BOSS DR11 LOWZ sample [32], the anisotropic measurement of D_A/r_d and $H r_d$ at $z = 0.57$ from the BOSS DR11 CMASS sample [32], and the improved measurements of D_V/r_s at $z = 0.44, 0.60, 0.73$ from the WiggleZ Dark Energy Survey [33]. Here r_d is the comoving sound horizon at the “drag” epoch when the baryons are “released” from the drag of the photons [34], and D_V is a volume averaged distance indicator similar to the angular diameter distance D_A [35].
- The Hubble constant measurement $H_0 = 73.8 \pm 2.4 \text{ km/s/Mpc}$ from the WFC3 on the HST (Hubble Space Telescope) [36].
- The high-redshift BAO measurement from the Quasar-Ly α -forest cross-correlation of the BOSS DR11 of SDSS-III [37], namely $\alpha_{\parallel}^{0.7} \alpha_{\perp}^{0.3} = 1.025 \pm 0.021$; α_{\parallel} and α_{\perp} are

¹It should be mentioned that, previous studies on the SNLS3 data sets [17] found strong evidence for the redshift-dependence of color-luminosity parameter β , and this conclusion has significant effects on parameter estimation of various cosmological models [18–21]. In addition, different light-curve fitters of SNIa can also affect the results of cosmology-fits [22–24]. But in this work, for simplicity, we just adopt the most mainstream recipe of processing SNLS3 data and do not consider the factors of time-varying β and different light-curve fitters.

Table 1. Fitting results for the Λ HDE model

Parameter	Planck + SNLS3 + BAO + HST		Planck + SNLS3 + BAO + HST + SDSS – Ly α	
	Best fit	68.3% limits	Best fit	68.3% limits
$\Omega_m h^2$	0.1405	$0.1413^{+0.0025}_{-0.0025}$	0.1375	$0.1400^{+0.0025}_{-0.0025}$
H_0	73.3	$70.5^{+1.3}_{-1.4}$	71.6	$70.5^{+1.3}_{-1.4}$
d	0.003	$0.570^{+0.320}_{-0.180}$	0.001	$0.308^{+0.075}_{-0.308}$
$\Omega_{\Lambda 0}$	0.61	$0.07^{+0.61}_{-0.14}$	0.63	$0.42^{+0.25}_{-0.10}$
Ω_{k0}	-0.0012	$0.0037^{+0.0037}_{-0.0059}$	-0.0063	$-0.0013^{+0.0028}_{-0.0032}$
χ^2_{min}	426.27		431.79	

defined as $\alpha_{\parallel} = \frac{[D_H(\bar{z})/r_d]}{[D_H(\bar{z})/r_d]_{\text{fid}}}$, $\alpha_{\perp} = \frac{[D_A(\bar{z})/r_d]}{[D_A(\bar{z})/r_d]_{\text{fid}}}$, where $\bar{z} = 2.34$, the fiducial values $[D_H(\bar{z})/r_d]_{\text{fid}}$ and $[D_A(\bar{z})/r_d]_{\text{fid}}$ are 8.708 and 11.59 respectively.

In the following context, we will use “SNLS3”, “Planck”, “BAO”, “HST” and “SDSS – Ly α ” to represent these five datasets.

We combine the above data sets to perform χ^2 analyses. Since SNLS3, Planck, BAO, HST and SDSS-Ly α are effectively independent measurements, the total χ^2 function is just the sum of all individual χ^2 functions:

$$\chi^2_{\text{total}} = \chi^2_{\text{SNLS3}} + \chi^2_{\text{Planck}} + \chi^2_{\text{BAO}} + \chi^2_{\text{HST}} + \chi^2_{\text{SDSS-Ly}\alpha}. \quad (3.3)$$

In our work, for a detailed investigation, we do fittings with two datasets: Planck + SNLS3 + BAO + HST and Planck + SNLS3 + BAO + HST + SDSS – Ly α , respectively.

The Λ HDE model has two dark energy parameters d , and Ω_{Λ} . Including four other cosmological parameters $\Omega_m h^2$, ω_b , Ω_k and h , and two nuisance parameters α , β characterizing the systematic errors of the SNLS3 dataset [13], the full set of free parameters in our analysis is

$$\mathbf{P} = \{\Omega_m h^2, \omega_b, h, c, \Omega_{\Lambda}, \Omega_k, \alpha, \beta\}. \quad (3.4)$$

In this work, we numerically solve Eq.(2.16) and Eq.(2.17) to obtain background evolutions of the Λ HDE model. The values of Ω_{r0} , for simplicity, are determined from the 7-yr WMAP observations [38],

$$\Omega_{r0} = \Omega_{\gamma 0}(1 + 0.2271N_{eff}), \quad \Omega_{\gamma 0} = 2.469 \times 10^{-5}h^{-2}, \quad N_{eff} = 3.046, \quad (3.5)$$

where γ represents photons, and N_{eff} is the effective number of neutrino species.

We modify the public available CosmoMC package [39] to explore the parameter space using the Markov Chain Monte Carlo (MCMC) algorithm. All the parameters listed in Eq. (3.4) are fitted simultaneously.

4 Dynamical Behaviors and the Cosmic Expansion History

4.1 Fitting Results

In Table 1, we give best-fit parameters as well as 68.3% confidence limits for constrained parameters. The results show that the spatial curvatures are close to zero in both cases (the 68.3% confidence limits are $|\Omega_{k0}| < 0.007$ and $|\Omega_{k0}| < 0.004$, respectively). Thus the results are impressively consistent with a spatially flat universe. Table 1 also gives the constraint on the parameter $\Omega_{\Lambda 0}$:

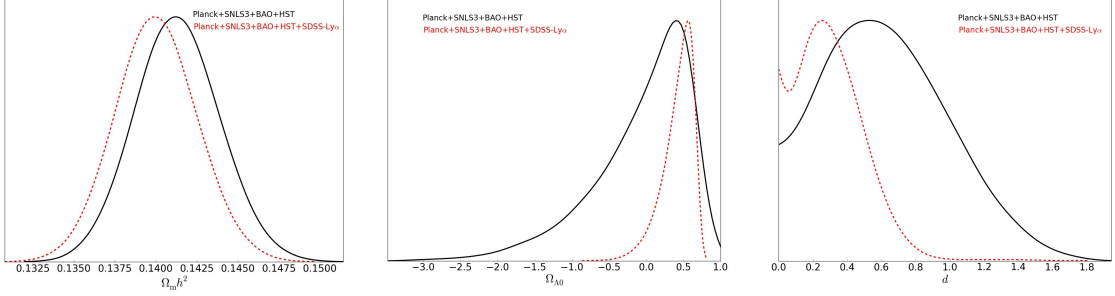


Figure 2. Marginalized likelihood distribution of $\Omega_m h^2$, $\Omega_{\Lambda 0}$, d constrained by Planck + SNLS3 + BAO + HST (solid lines) and Planck + SNLS3 + BAO + HST + SDSS – Ly α (dashed lines) datasets.

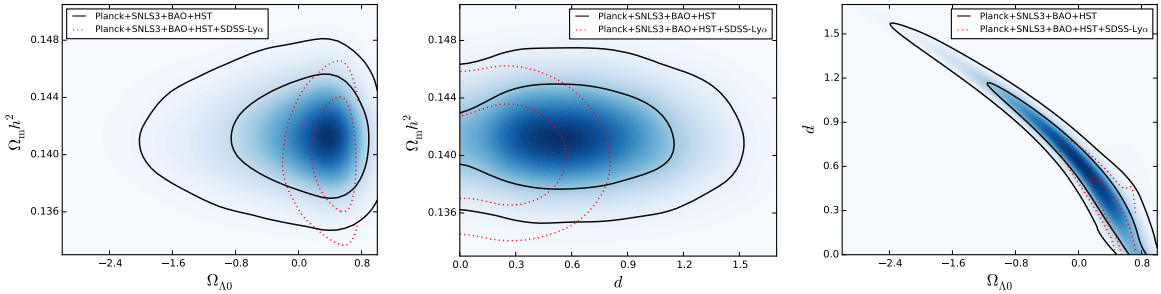


Figure 3. Marginalized 68.3% and 95.4% CL contours of $\Omega_{\Lambda 0}$ - $\Omega_m h^2$, d - $\Omega_m h^2$ and $\Omega_{\Lambda 0}$ - d planes constrained by Planck + SNLS3 + BAO + HST (solid lines) and Planck + SNLS3 + BAO + HST + SDSS – Ly α (dotted lines) datasets.

Planck + SNLS3 + BAO + HST: $-0.07 < \Omega_{\Lambda 0} < 0.68$ (68.3% CL);

Planck + SNLS3 + BAO + HST + SDSS – Ly α : $0.32 < \Omega_{\Lambda 0} < 0.67$ (68.3% CL).

Combine with the constraint results of $\Omega_m h^2$ and H_0 listed in Table 1 together, we get the corresponding constraint on Ω_{hde0} :

Planck + SNLS3 + BAO + HST: $0.04 < \Omega_{hde0} < 0.79$ (68.3% CL);

Planck + SNLS3 + BAO + HST + SDSS – Ly α : $0.06 < \Omega_{hde0} < 0.41$ (68.3% CL).

Fig. 2 shows the marginalized likelihood distributions of parameter d , $\Omega_m h^2$ and $\Omega_{\Lambda 0}$ constrained by Planck+SNLS3+BAO+HST and Planck+SNLS3+BAO+HST+SDSS–Ly α datasets, respectively. The 68.3% and 95.4% contours of $\Omega_{\Lambda 0}$ - $\Omega_m h^2$, d - $\Omega_m h^2$ and $\Omega_{\Lambda 0}$ - d planes are plotted in Fig. 3.

The results show that, compared with the Planck + SNLS3 + BAO + HST dataset, the Planck + SNLS3 + BAO + HST + SDSS – Ly α dataset makes a more tighter constraints on d and $\Omega_{\Lambda 0}$ parameters. We also find that a smaller value of $\Omega_m h^2$ and a bigger value of $\Omega_{\Lambda 0}$ is favored by the Planck + SNLS3 + BAO + HST + SDSS – Ly α dataset.

Table 2. The χ^2_{\min} s, ΔAICs and ΔBICs of the ΛCDM , HDE and ΛHDE models, obtained by using the Planck + SNLS3 + BAO + HST and Planck + SNLS3 + BAO + HST + SDSS – Ly α datasets, respectively.

Model	Planck + SNLS3 + BAO + HST			Planck + SNLS3 + BAO + HST + SDSS – Ly α		
	χ^2_{\min}	ΔAIC	ΔBIC	χ^2_{\min}	ΔAIC	ΔBIC
ΛCDM	431.35	0	0	438.22	0	0
HDE	428.20	–1.15	3.03	438.19	1.97	6.15
ΛHDE	426.27	–1.06	7.27	431.79	–2.43	5.92

There is a degeneracy between d and $\Omega_{\Lambda 0}$, which can be seen in Fig. 3. The reason is that both the cosmological constant and HDE are good candidate for explaining the feature of cosmic acceleration revealed by current observational data. Therefore, when we combine the HDE and cosmological constant components together (thus ΛHDE model), we may probably get the degeneracy.

In addition to the cosmological consequence of the ΛHDE model, we are also interested in its comparison with the ΛCDM and the original HDE models. Therefore we also perform the χ^2 analysis of the ΛCDM and the HDE models by using the same datasets. To assess different models, here we adopt the Akaike information criteria (AIC) [40] and Bayesian information criteria (BIC) [41], defined as

$$\text{AIC} = \chi^2_{\min} + 2k, \quad \text{BIC} = \chi^2_{\min} + k \ln N, \quad (4.1)$$

where k is the number of free parameters, and N is the number of data points used in the fits. A model with smaller AIC (BIC) is more favored.

Table 2 shows the χ^2_{\min} s, AICs and BICs of the ΛCDM , HDE and ΛHDE models. Notice that the values of the AIC and BIC themselves are not interesting, thus we only list the difference between the ΛHDE (HDE) and ΛCDM models, i.e.,

$$\Delta\text{AIC}_{\text{model}} \equiv \text{AIC}_{\text{model}} - \text{AIC}_{\Lambda\text{CDM}}, \quad \Delta\text{BIC}_{\text{model}} \equiv \text{BIC}_{\text{model}} - \text{BIC}_{\Lambda\text{CDM}} \quad (4.2)$$

Compared with the ΛCDM and HDE models, the ΛHDE model provides a better fit to the data. For Planck + SNLS3 + BAO + HST dataset, the ΛHDE model reduces the χ^2_{\min} s by amount of 5.08 (1.93) compared with the ΛCDM (HDE) model. While for Planck + SNLS3 + BAO + HST + SDSS – Ly α dataset, the ΛHDE model reduces the χ^2_{\min} s by amount of about 6.4 compared with the other two models. By adopting the AIC and BIC, Table 2 also shows that, compared with ΛCDM model, the ΛHDE model is slightly favored by AIC. But both the ΛHDE and HDE models are not favored by BIC, though these models have slightly smaller χ^2_{\min} s than the ΛCDM model.

4.2 The Expansion History

It is worth investigating the cosmic expansion history of the ΛHDE model by the fitting results.

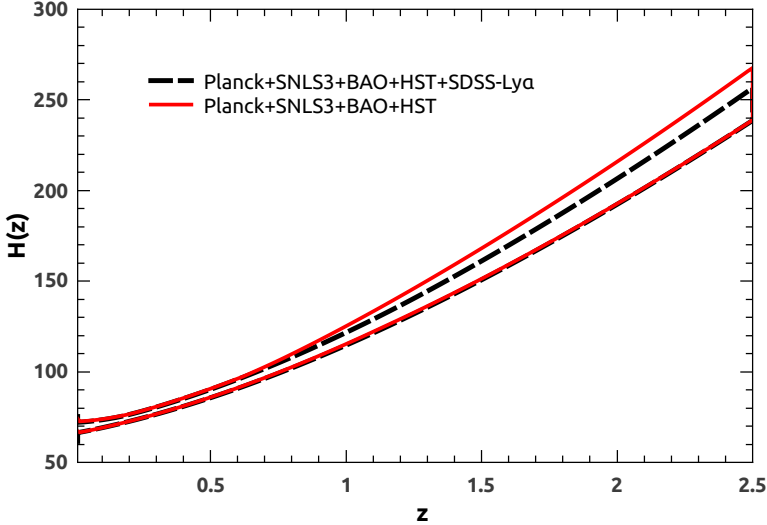


Figure 4. Reconstructed evolution history of $H(z)$ (95.4% CL) in Λ HDE model, constrained by the Planck + SNLS3 + BAO + HST (red solid lines) and Planck + SNLS3 + BAO + HST + SDSS – Ly α (black dashed lines) datasets respectively.

In Fig. 4, we plot the reconstructed evolution history of $H(z)$ (95.4% CL) in Λ HDE model, constrained by the Planck + SNLS3 + BAO + HST and Planck + SNLS3 + BAO + HST + SDSS – Ly α datasets, respectively. We find that, in low redshift region, the reconstructed evolution history $H(z)$ of the Planck + SNLS3 + BAO + HST and Planck + SNLS3 + BAO + HST + SDSS – Ly α datasets are almost the same. However, in the high redshift region, the constraint of the Planck + SNLS3 + BAO + HST + SDSS – Ly α dataset is much more tighter than that of the Planck + SNLS3 + BAO + HST dataset. It is clear that this feature is due mainly to the SDSS-Ly α data at redshift $z = 2.34$. As revealed by [42, 43], the high redshift datasets play a big part in constraining the cosmic expansion history.

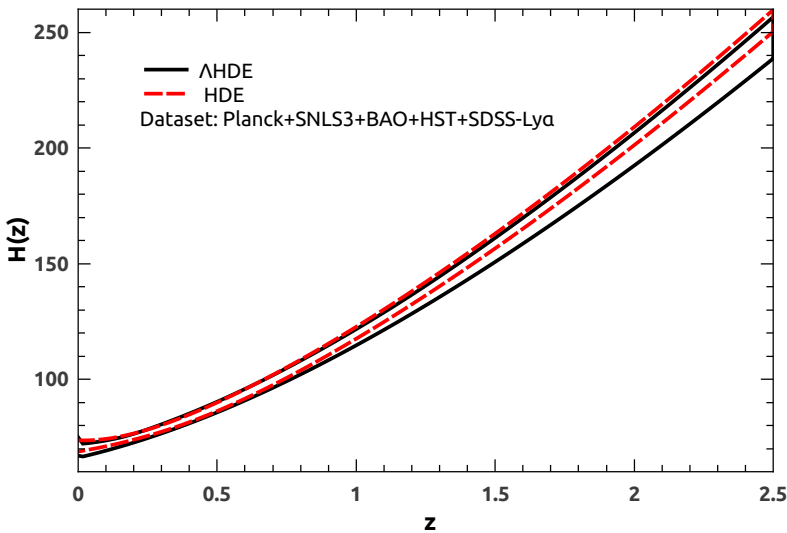


Figure 5. Reconstructed evolution history of $H(z)$ (95.4% CL) constrained by Planck + SNLS3 + BAO + HST + SDSS – Ly α dataset in Λ HDE model(black solid lines) . The corresponding results for HDE model is also plotted (red dashed lines) for comparison.

For a comparison, it is also of value to compare the Λ HDE model with the original HDE model. Fig. 5 shows the reconstructed evolution history of $H(z)$ (95.4% CL) in the Λ HDE and the original HDE model constrained by Planck + SNLS3 + BAO + HST + SDSS – Ly α dataset. We find that the reconstructed $H(z)$ of Λ HDE and HDE models have negligible difference in the low redshift region. However, in the high redshift region, the $H(z)$ in Λ HDE model has slightly lower value, which should be due mainly to the existence of a cosmological constant component in the model.

4.3 Equation of State

In this subsection we discuss the EoS w , which is believed to be the most important marker of the properties of dark energy.

Fig. 6 shows the reconstructed evolution history of $w(z)$ at $0 \leq z \leq 2.5$ (68.3% and 95.4% CL) constrained by Planck + SNLS3 + BAO + HST + SDSS – Ly α dataset. It shows that w slightly cross -1 from above roughly at the current epoch. However, in the past we have w slightly bigger than -1, which can be viewed as a feature of diluted holographic dark energy. This behavior is consistent with the results shown by Fig. 5.

As mentioned above, the dynamical evolution of dark energy have not be confirmed by the current observational data. Our results is consistent with this statement.

From Fig. 4, we can conclude that, if we want to break the degeneracy between the HDE and cosmological constant components, one way is to get more observational data at high redshifts.

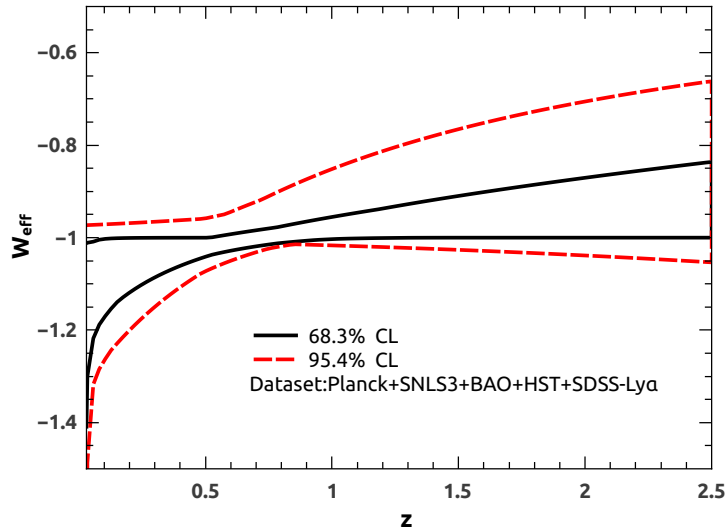


Figure 6. Reconstructed evolution history of $w(z)$ at 68.3% (black solid lines) and 95.4% (red dashed lines) CL in Λ HDE model, constrained by the Planck + SNLS3 + BAO + HST + SDSS – Ly α dataset.

5 Conclusion

In this work, we study the Λ HDE model in which there are two parts, the first being the cosmological constant and the second being the holographic dark energy. This model has similar dynamical equations with the original HDE model, except a cosmological term. By studying the Λ HDE model theoretically, we find that the parameters d and Ω_{hde} are divided into a few domains in which the fate of the universe is quite different.

Using the Planck + BAO + SNLS3 + HST and Planck + BAO + SNLS3 + SDSS – Ly α datasets, we investigate the dynamical properties and cosmic expansion history of the Λ HDE model. The results shows that the goodness-of-fit of the Λ HDE model are $\chi^2_{\min}=426.27$ (Planck+SNLS3+BAO+HST) and $\chi^2_{\min}=431.79$ (Planck+SNLS3+BAO+HST+SDSS–Ly α) which is smaller then the results of the original HDE model (Planck + SNLS3 + BAO + HST:428.20; Planck + SNLS3 + BAO + HST + SDSS – Ly α :438.19) and the concordant Λ CDM model (Planck + BAO + SNLS3 + HST:431.35; Planck + SNLS3 + BAO + HST + SDSS – Ly α :438.22) obtained using the same datasets. Especially when constrained by the Planck+SNLS3+BAO+HST+SDSS–Ly α dataset, The χ^2_{\min} of Λ HDE model shrinks more than 6, compared with both the HDE and Λ HDE model. Thus, the Λ HDE model provides a nice fit to the cosmological data.

For parameter $\Omega_{\Lambda 0}$, the 68.3% confidence level constrained by the Planck + SNLS3 + BAO + HST and the Planck + SNLS3 + BAO + HST + SDSS – Ly α dataset is $-0.07 < \Omega_{\Lambda 0} < 0.68$ and $0.32 < \Omega_{\Lambda 0} < 0.67$, respectively. This gives the corresponding components of the holographical dark energy, namely

$$\text{Planck + BAO + SNLS3 + HST: } 0.04 < \Omega_{hde0} < 0.79;$$

$$\text{Planck + SNLS3 + BAO + HST + SDSS – Ly}\alpha: 0.06 < \Omega_{hde0} < 0.41.$$

We also find that there is degeneracy between the cosmological constant and the holographic dark energy component when constrained by current cosmological observations. By reconstructing the evolution of the EoS of dark energy, we find the Λ HDE mainly differs from the original HDE model at high redshift (as shown in Fig.5).

From the constraint results by Planck + SNLS3 + BAO + HST + SDSS – Ly α dataset, it shows that if we want to break the degeneracy between the HDE and cosmological constant components, one way is to get more observational data at high redshifts.

Acknowledgments

We are grateful to the Referee for the valuable suggestions. We also thank Xiao-Dong Li and Shuang Wang for their helps on fitting issues. ML is supported by the National Natural Science Foundation of China (Grant No. 11275247, and Grant No. 11335012) and 985 grant at Sun Yat-Sen University.

6 Appendix: Proof for $\log a$ not having a maximum in Λ HDE model

In this appendix, we prove that x does not have a maximum as a function of time. Since x does not have a maximum in either Λ CDM or HDE model, here we only consider Λ HDE model, which includes the coexistence case of HDE and cosmological constant.

In a flat universe, the Friedmann equation is

$$3M_{pl}^2 H^2 = \rho_{dm} + \rho_b + \rho_r + \rho_\Lambda + \rho_{hde}, \quad (6.1)$$

Let us note that

$$g(x) = \frac{d}{dx} \ln |f(a)|, \quad (6.2)$$

$$\text{then } g(x) = \frac{2\Omega_{\Lambda 0}e^{2x} - \Omega_{m0}e^{-x} - 2\Omega_{r0}e^{-2x}}{\Omega_{\Lambda 0}e^{2x} + \Omega_{m0}e^{-x} + \Omega_{r0}e^{-2x}}. \quad (6.3)$$

According to Eq.(2.25), we get

$$\frac{d\Omega_{hde}}{dx} = [\frac{2}{d}\sqrt{\Omega_{hde}} - g(x)]\Omega_{hde}(1 - \Omega_{hde}). \quad (6.4)$$

We first consider the cases that $\Omega_{\Lambda 0} > 0$ or $\Omega_{\Lambda 0} + \Omega_{m0} + \Omega_{r0} < 0$. In these cases, $g(x)$ is a bounded function in the region $(x_0, +\infty)$. If x has a maximum x_m , H would approach zero when x goes to x_m . According to Eq.(6.1), Ω_{hde} would approach infinity. However, Eq.(6.4) shows that, once $\sqrt{\Omega_{hde}} > \frac{d}{2}g(x)$ and $\Omega_{hde} > 1$, $\frac{d}{dx}\sqrt{\Omega_{hde}} < 0$. Thus Ω_{hde} would never approach infinity. So x has no maximum in these cases.

Another case is $\Omega_{\Lambda 0} < 0$ and $\Omega_{\Lambda 0} + \Omega_{m0} + \Omega_{r0} > 0$. In this case

$$\exists x_c > 0 : \Omega_{\Lambda 0}e^{2x_c} + \Omega_{m0}e^{-x_c} + \Omega_{r0}e^{-2x_c} = 0. \quad (6.5)$$

So Eq.(6.4) has a singularity at $x = x_c$. Similar to the previous analysis, x does not have a maximum in the region (x_0, x_c) . Now we prove that x_c is not a maximum of x . If it is, $g(x)$ would approach negative infinity and Ω_{hde} would approach infinity when x goes to x_c . However, once $\Omega_{hde} > 1$, $\frac{d}{dx}\sqrt{\Omega_{hde}} < 0$. Thus Ω_{hde} would never approach infinity. So x_c is not a maximum of x . When $x > x_c$, we can see that $\Omega_{\Lambda} + \Omega_m + \Omega_r < 0$. This is just the case we have discussed. So x also has not a maximum when $x > x_c$.

In summary, we have proved that x does not have a maximum. So we can use a constant k_r to approximate $\frac{d}{dx} \ln |f(a)|$ when we study the fate of the universe.

References

- [1] A. Cohen, D. Kaplan, A. Nelson, Phys. Rev. Lett. **82**, 4971 (1999).
- [2] M. Li, Phys. Lett. B **603**, 1 (2004).
- [3] G. 't Hooft, gr-qc/9310026; L. Susskind, J. Math. Phys. **36**, 6377 (1995); J. D. Bekenstein, Phys. Rev. D **7**, 2333 (1973); J. D. Bekenstein, Phys. Rev. D **9**, 3292 (1974); J. D. Bekenstein, Phys. Rev. D **23**, 287 (1981); J. D. Bekenstein, Phys. Rev. D **49**, 1912(1994); S. W. Hawking, Commun. Math. Phys. **43**, 199 (1975); S. W. Hawking, Phys. Rev. D **13**, 191 (1976).
- [4] A. G. Riess *et al.*, AJ. **116**, 1009 (1998); S. Perlmutter *et al.*, ApJ. **517**, 565 (1999).
- [5] V. Sahni and A. Starobinsky, Int. J. Mod. Phys. **D9**, 373 (2000); P. J. E. Peebles and B. Ratra, Rev. Mod. Phys. **75**, 559 (2003); T. Padmanabhan, Phys. Rept. **380**, 235 (2003); E. J. Copeland, M. Sami and S. Tsujikawa, Int. J. Mod. Phys. D **15**, 1753 (2006); V. Sahni and A. Starobinsky, Int. J. Mod. Phys. **D15**, 2015 (2006); J. Frieman, M. Turner and D. Huterer, Ann. Rev. Astron. Astrophys. **46**, 385 (2008); S. Tsujikawa, arXiv:1004.1493; M. Li *et al.*, Commun. Theor. Phys. **56**, 525 (2011); M. Li *et al.*, arXiv:1209.0922.
- [6] M. Li, C. S. Lin and Y. Wang, JCAP **0805**, 023 (2008).
- [7] Q. G. Huang and Y. G. Gong, JCAP 0408, 006 (2004); X. Zhang and F. Q. Wu, Phys. Rev. D **76**, 023502 (2007); M. Li, X. D. Li, S. Wang and X. Zhang, JCAP 0906, 036 (2009).

[8] C. J. Hogan, astro-ph/0703775; arXiv:0706.1999; Q. G. Huang and M. Li, JCAP **0503**, 001 (2005); X. Zhang, Int. J. Mod. Phys. D **14**, 1597 (2005); Phys. Lett. B **648**, 1 (2007); Phys. Rev. D **74**, 103505 (2006); B. Chen, M. Li and Y. Wang, Nucl. Phys. B **774**, 256 (2007); J. F. Zhang, X. Zhang and H. Y. Liu, Phys. Lett. B **651**, 84 (2007); H. Wei and S. N. Zhang, Phys. Rev. D **76**, 063003 (2007); Y. Z. Ma and X. Zhang, Phys. Lett. B **661**, 239 (2008); M. Li *et al.*, Commun. Theor. Phys. **51**, 181 (2009); B. Nayak and L. P. Singh, Mod. Phys. Lett. A **24**, 1785 (2009); K. Y. Kim, H. W. Lee and Y. S. Myung, Mod. Phys. Lett. A **24**, 1267 (2009); M. Li, R. X. Miao and Y. Pang, Phys. Lett. B **689**, 55 (2010); M. Li, R. X. Miao and Y. Pang, Opt. Express **18**, 9026 (2010); M. Li and Y. Wang, Phys. Lett. B **687**, 243 (2010); Y. G. Gong and T. J. Li, Phys. Lett. B **683**, 241 (2010); L. N. Granda, A. Oliveros and W. Cardona, Mod. Phys. Lett. A **25**, 1625 (2010); Z. P. Huang and Y. L. Wu, arXiv:1202.4228.

[9] M. Li, R. X. Miao and Y. Pang, Phys. Lett. B **689**, 55 (2010); M. Li, R. X. Miao and Y. Pang, Opt. Express **18**, 9026 (2010).

[10] Zhang Z et al. Revist of the Interaction between Holgraphic Dark Energy and Dark Mater. JCAP, 06(2012) 09.

[11] Q. G. Huang and M. Li, JCAP **0408**, 013 (2004).

[12] M. Li, R. X. Miao, arXiv:1210.0966.

[13] Guy J et al. The Supernova Legacy Survey 3-year sample: Type Ia supernovae photometric distances and cosmological constraints. A&A, 2010, 523, A7.

[14] Sullivan M et al. SNLS3: Constraints on Dark Energy Combining the Supernova Legacy Survey Three-year Data with Other Probes. ApJ, 2011, 737, 102.

[15] Conley A J et al. SiFTO: An Empirical Method for Fitting SN Ia Light Curves. ApJ, 2008, 681 : 482-498.

[16] Guy J et al. SALT2: using distant supernovae to improve the use of type Ia supernovae as distance indicators. A&A, 2007, 466:11-21.

[17] Wang, S.; Wang, Y., 2013, Phys. Rev. D 88, 043511.

[18] Wang, S.; Li, Y.-H.; Zhang, X. 2014, Phys. Rev. D 89, 063524.

[19] Wang, S.; Wang, Y.-Z.; Geng, J.-J.; Zhang X. 2014, Eur. Phys. J. C 74, 3148.

[20] Wang, S.; Wang, Y.-Z.; Zhang X. 2014, Commun. Theor. Phys. 62, 927.

[21] Wang, S.; Geng, J.-J.; Hu, Y.-L.; Zhang X., 2015, Sci. China Phys. Mech. Astron. 58, 019801.

[22] Bengochea, G. R., 2011, Phys. Lett. B 696, 5.

[23] Bengochea, G. R., & De Rossi, M. E., 2014, Phys. Lett. B 733, 258.

[24] Hu, Y.-Z.; Li, M.; Li, N.; Wang, S., 2015, arXiv:1501.06962.

[25] Zhang Z H et al. Generalized Holographic Dark Energy and its Observational Constraints. Mod. Phys. Lett. A 2012, 27, 1250115.

[26] Wang Y, Wang S. Distance priors from Planck and dark energy constraints from current data. Phys. Rev. D, 2013, 88, 043522.

[27] Ade P A R et al. Planck 2013 results. I. Overview of products and scientific results. arXiv:1303.5062.

[28] Ade P A R et al. Planck 2013 results. XVI. Cosmological parameters. arXiv:1303.5076.

[29] Hu W, Sugiyama N. Small-Scale Cosmological Perturbations: An Analytic Approach. ApJ, 1996, 471 : 542-470.

[30] Li M et al. Dark Energy. Commun.Theor.Phys., 2011, 56:525-604.

- [31] Beutler F. et al. The 6dF Galaxy Survey: baryon acoustic oscillations and the local Hubble constant. MNRAS, 2011, 416 : 3017-3032.
- [32] Anderson L. et al. The clustering of galaxies in the SDSS-III Baryon Oscillation Spectroscopic Survey: Baryon Acoustic Oscillations in the Data Release 10 and 11 galaxy samples. arXiv:1312.4877.
- [33] Kazin E A et al. Improved WiggleZ Dark Energy Survey Distance Measurements to $z = 1$ with Reconstruction of the Baryonic Acoustic Feature. arXiv:1401.0358.
- [34] Eisenstein D J, Hu W. Baryonic Features in the Matter Transfer Function. ApJ, 1998, 496 : 605-614.
- [35] Eisenstein D J et al. Detection of the Baryon Acoustic Peak in the Large-Scale Correlation Function of SDSS Luminous Red Galaxies. ApJ, 2005, 633 : 560-574.
- [36] Riess A G et al. A 3% Solution: Determination of the Hubble Constant with the Hubble Space Telescope and Wide Field Camera 3. ApJ, 2011, 730, 119.
- [37] Delubac, T. et al. A &A 574, A59 (2015), arXiv:1404.1801.
- [38] Komatsu E et al. Seven-year Wilkinson Microwave Anisotropy Probe (WMAP) observations: cosmological interpretation. ApJ Suppl., 2011, 192 : 18-64.
- [39] Lewis A, Bridle S. Cosmological parameters from CMB and other data: A Monte Carlo approach. Phys. Rev. D, 2002, 66, 103511.
- [40] H. Akaike, IEEE Trans. Automatic Control **19**, 716 (1974).
- [41] G. Schwarz, Ann. Stat. **6**, 461 (1978).
- [42] Sahni,V. et al., 2014 , Astrophys.J. 793 (2014) L40.
- [43] Hu,Y. et al., 2014 , arXiv:1406.7695.